An Investigation of the Contribution of the Multi-Joint Arm Stiffness to the Motor Control Defecit experienced in Ataxia

by

Olumuyiwa A. Oni

Submitted to the Department of Mechanical Engineering
in Partial Fulfillment of the
Requirements for the Degree of

Bachelors of Science

at the

Massachusetts Institute of Technology

June 2006-05-26

Signature of Author ....
Department of Mechanical Engineering
May 26, 2006-05-26

Certified by ....
Steve Massaquoi
Assistant Professor of EECS and HST
Thesis Supervisor

Accepted by ....
Professor John H. Lienhard V
Chairman of the Undergraduate Thesis Committee

An Investigation of the Contribution of the Multi-Joint Arm Stiffness to the Motor Control Defect experienced in Ataxia

by

Olumuyiwa A. Oni

Submitted to the Department of Mechanical Engineering
on May 25, 2006 in partial fulfillment of the
requirements for the Degree of Bachelors of Science in
Mechanical Engineering

ABSTRACT

Prior research has shown that the control response of the limbs is affected by the mechanical properties of the limb and the feedback properties of the CNS. Cerebellar ataxia describes a situation in which damage to the cerebellum results in compromised motor control. It is characterized by such things as a clumsy or disturbed gait, a lack of balance and coordination, and unsteady speech patterns; for severe cases of ataxia, gross muscle coordination can degenerate to the point where successful, coordinated movements are not possible. In order to better understand the control deficit experienced by ataxic persons, estimates of the feedback properties of the CNS and the limb-muscle mechanical properties and will be necessary. Specifically, this investigation hopes to determine to what extent ataxia is cause by abnormal effective stiffness. Because ataxic patients do not exhibit deficits in strength or postural maintenance, we hypothesize a priori that the measured stiffness of ataxic subjects will be normal. We test this by conducting postural stiffness study on an ataxic subject, and measuring stiffness for two degrees of subject co-activation – minimal subject co-activation and maximal subject co-activation – and for different equilibrium postures. Because the observed kinematic trajectory following neuromuscular activation, as well as the ability of the limb to maintain a given posture in an external force field will be a result of the CNS reflex responses as well as the mechanical properties of the limb-muscle system, we expect all measurements of stiffness to be affected by CNS reflex responses. These reflex responses tend to be noticed between 20 msec (spinal reflexes) and 150 msec (long-loop reflexes) after an environmental disturbance, and because measurements of muscle stiffness require that we wait at least that long after external force application, we expect their contribution to the stiffness measurements to be represented.
Our findings show the postural stiffness measured at six static positions in a 0.23 meter by 0.23 meter horizontal workspace and centered 0.45 m in front of the ataxic subject were within (something %) of those measured for a normal subject, and within the range reported by Mussa-Ivaldi. As expected, however, the kinematics of cross-body hand movements were significantly different for the ataxic and normal subject. These results indicate an intact postural regulation for the ataxic subject but a deficit in dynamic control when compared to the normal subject.

Thesis Supervisor: Steve Massaquoi

Title: Assistant Professor of Electrical Engineering and Computer Science and Health-Science and Technology

1.0 Introduction:

When the hand is displaced from an equilibrium posture by an external force, a force is generated to restore the initial position. According to the equilibrium point hypothesis, the force generated is dependent on the posture, mechanical properties of muscles, and the response of the CNS. This study measured the postural, multi-joint arm stiffness for an ataxic and a normal subject at several defined points in a horizontal workspace and under two conditions: when the subject's muscles were relaxed and during co-contraction. The Experimental apparatus consisted of a two-joint manipulandum, two torque motors connected independently to each joint, high resolution position transducers co-located on the motors, a force transducer mounted at the handle and an LCD screen with a live image representing the hand's position in the pre-defined workspace. The apparatus was capable of supporting the subject's arm in a horizontal plane and applying controlled amplitude and direction force to the subject hand. During the study, a subject would locate his hand at a position in the workspace corresponding to a target shown on the LCD screen. A controlled force would then be applied at the hand of the subject and the resulting displacement would be measured. In order to prevent visual correction during force application, visual feedback of the hand position was stopped just before the force was initiated. With force-displacement measurements at the pre-defined targets in the workspace we were able to investigate the differences in the joint stiffness properties for the ataxic and normal subject – such as the orientation, magnitude and ratio of maximal and minimal stiffness direction. Using the same apparatus, a second study comparing arm dynamics during point-to-point cross-body movements was conducted. The subject would work in the same workspace, but under a force field that effectively cancelled the dynamics of the manipulandum. He would locate his hand at the position in the work space corresponding to one target of a target pair shown on the LCD screen and complete point to point movements, from one target to the next and back at a range of speeds.

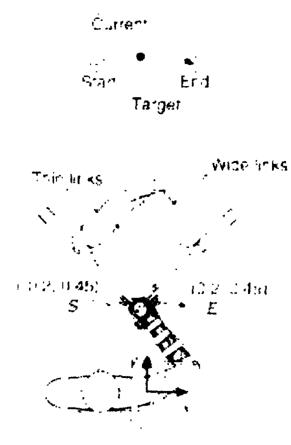

Figure 1. Manipulandum Schematic.[1]

[1] Figure from Gomi & Kawato

2.0 **Relevant Theory:**

2.1 Equilibrium Point Hypothesis:

If we took the biomechanical model of the two-joint arm, illustrated in Figure 2, and replace each antagonistic muscle group with a pair of opposing springs, the arm would tend to settle to the same configuration regardless of where it was released. This configuration is the equilibrium point of the system, and this would change depending on the length-tension properties of the springs – by changing the spring's resting lengths or stiffnesses, the equilibrium point of the system would change. Several studies have suggested that the length-tension properties of human muscle are similar to that of springs in that the static force they generate depends on length. (Bizzi, McIntyre) In fact, according to the equilibrium point hypothesis, multi-joint limb configuration is determined by the length-tension properties of the muscles. Experimental investigations of the role of muscle mechanical properties in motor control have suggested that a muscle is mechanically analogous to a "tunable" spring, i.e. it is characterized by a set of integrable functions between length and tension at steady state. (Lan) The equilibrium position and the stiffness of a joint would be defined, for any given value of muscle activation, as the position at which the length-dependent forces of opposing muscles generate equal and opposite torques about the joint. This view of posture has been extended to the analysis of movement and trajectory formation.

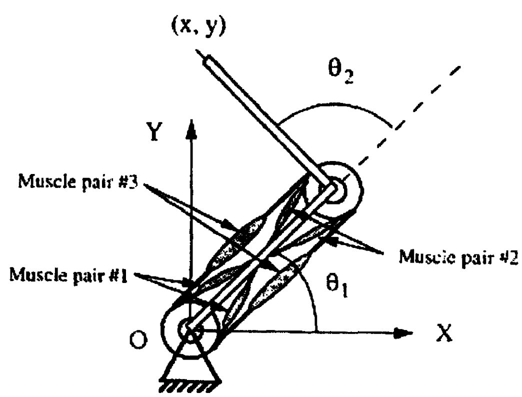

Figure 2. Two-joint arm model. Three pairs of antagonist muscles are included: *pair #1* is shoulder muscles, *pair #2* is elbow muscles, *pair #3* is biarticular muscles.[2]

2.2 Previous Work:

Studies conducted by Mussa-Ivaldi (1985) sought to characterize the mechanical and geometrical factors involved in maintaining arm posture during external force application. This study found that that the shape and orientation of the maximal and

[2] Figure from.

minimal stiffness were invariant over subjects and over time though the magnitude did vary.. The convention established by Mussa-Ivaldi represented postural multi-joint stiffness graphically as an ellipse characterized by three parameters: the magnitude (the area), the shape (the ratio of axis) and the orientation (direction of major axis). A follow-up studies conducted by Flash (1987) applied the results of the Mussa-Ivaldi study to test the validity of the equilibrium trajectory hypothesis. Flash proposed that multi-joint arm movements are achieved by shifting the equilibrium positions defined by neuromuscular activity along a straight line. This view has been widely disproved by investigations that suggest: 1) the actual stiffness values reported by Flash were incorrect (Gomi); and 2) That the Flash model does not account for learning and inverse dynamics, and that the learning was addressed, in large part, by the cerebellum (Kawato). For the same reasons the Flash model widely disproved as an accurate general model of point-to-point kinematic limb trajectory, it may be a reasonable model to describe the reaching movements of subjects with damaged cerebellums.

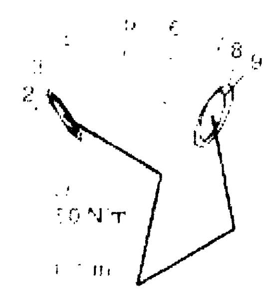

Figure 3. Mussa-Ivaldi, changes in stiffness induced by changes in arm configuration.

2.3 Relevant Equations:

Joint Torque to Displacement:

The mechanical links of the manipulandum are constrained to move in a horizontal plane only. When a joint at one end of a mechanical link is subject to an unbalanced torque, the link will experience an angular displacement, $\Delta\theta$, about the center of rotation of the joint. The free end of the mechanical link will experience a corresponding linear displacement given by

$$dx = L*\cos(\Delta\theta)$$
$$dy = L*\sin(\Delta\theta) \qquad (1)$$

where dx and dy are respectively, the imposed displacement in the x and y directions, and L is the length of the link from the axis of rotation of one joint to the free tip (or, if applicable, to the axis of rotation of next joint). In order to determine a reference position of the free end of a mechanical link, it is necessary to specify a reference origin and reference direction corresponding to the 0 angle. For example, for a coordinate system in the frame of the manipulandum, the origin was set as the intersection of axis of rotation of the torque motors and the horizontal plane of the manipulandum, and the reference 0 angle of the proximal joint was set parallel to the direction of the distal link in the horizontal plane. (A reference 0 angle for the distal joint was arbitrarily chosen during the position calibration of the manipulandum.) The position of the proximal joint and the tip of the proximal link of the two-joint manipulandum in the reference coordinate system can be calculated by summing incremental linear and angular displacements (Eqn. 2), and will be given by

$$x_{tip} := L_1 \cdot \cos(\theta_1) + L_2 \cdot \cos(\theta_1 + \theta_2)$$
$$y_{tip} := L_1 \cdot \sin(\theta_1) + L_2 \cdot \sin(\theta_1 + \theta_2) \qquad (2)$$

where L_1 and L_2 are the manipulandum link lengths; θ_1 and θ_2 are respectively, the angle offset from a reference 0 direction of joint 1and at joint 2 ; x_{j2} and y_{j2}, and x_{tip} and y_{tip} are the x and y coordinates respectively, for the proximal joint and for the tip of the proximal link. respectively; x_{tip} and y_{tip} are the imposed displacement x and y directions, respectively.

Given the position of the subject's hand in the manipulandum's reference frame, we can approximate the joint angles of the subject in the subject reference frame if we know position of the origin of the subject's reference frame and the length of his forearm (specifically the distance between the centers of rotation of the shoulder and the elbow, and the distance between the center of rotation of the elbow and the handle). By rearranging Eqn. 2 in the coordinate system of the subject, we can solve for the offset angles, θ_1 and θ_2, using inverse kinematics; they will be given by

$$r := \sqrt{\left(x^2 + y^2\right)}$$

$$\theta_1 := \operatorname{atan2}(x, y) - \frac{\operatorname{acos}\left(\left(r^2 + L_1^{\,2} - L_2^{\,2}\right)\right)}{2 \cdot r \cdot L_1}$$

$$\theta_{2.} := \pi - \frac{\operatorname{acos}\left(\left(-r^2 + L_1^{\,2} + L_2^{\,2}\right)\right)}{2 \cdot L_1 \cdot L_2} \qquad (3)$$

where r is the distance from the origin.

Force and Torque:

The force experienced at the handle can be determined from the geometrical configuration of the two-joint manipulandum and measurements of the torques experienced at each joint. The transformation from torque to force will be given by

$$F_x := \left(\tau_1 \cdot \frac{\cos(\theta_1 + \theta_2)}{L_1} - \tau_2 \cdot \frac{\cos(\theta_1)}{L_2}\right) \cdot \sin(\theta_2)^{-1} \qquad (4)$$

$$F_y := \left(\tau_1 \cdot \frac{\sin(\theta_1 + \theta_2)}{L_1} - \tau_2 \cdot \frac{\sin(\theta_1)}{L_2} \right) \cdot \sin(\theta_2)^{-1}$$

where τ_1 and τ_2 are the torques being applied by the motors, and F_x and F_y are the forces applied at the handles in the x and y directions.

When a hand is displaced from its desired location, restoring forces are generated that attempt to return the desired location. These forces result from elastic properties of the spinal stretch reflexes (acting at around 30 msec delay) and slower transcortical reflexes. Together, these form an effective stiffness. This stiffness can be measure by applying a step in force to the hand, waiting for the limb to come to rest at its new location, and measuring the resulting displacement. The postural stiffness of the arm would be given by

$$F_x := -K_{xx} \cdot dx - K_{xy} \cdot dy$$

$$F_y := -K_{yx} \cdot dx - K_{yy} \cdot dy \qquad (5)$$

$$K := \begin{pmatrix} K_{xx} & K_{xy} \\ K_{yx} & K_{yy} \end{pmatrix}$$

where K_{xx}, K_{xy}, K_{yx} and K_{yy} represent the linear stiffnesses in the x and y directions. Physically, a larger K value indicates more a small resulting displacement in the direction of a given applied force. The K values representing linear force displacement should always be positive, because a positive force should result in a positive displacement. There are no restrictions on the sign of the off diagonal terms, however, they must be identical for the stiffness matrix to be conservative; this means that the force-displacement profile is spring-like and that for a closed path trajectory, the net Work produced in the muscle is zero. If the difference between the two off diagonal components is large, the curl is said to be non-negligible and the likelihood of observing tremors in movements becomes high). The stiffness matrix K can be broken down into conservative and non-conservative components.

$$K_{sym} := \begin{pmatrix} K_{xx} & \frac{K_{xy} + K_{yx}}{2} \\ \frac{K_{xy} + K_{yx}}{2} & K_{yy} \end{pmatrix}$$

$$K_{asym} := \begin{pmatrix} 0 & \frac{K_{xy} - K_{yx}}{2} \\ \frac{K_{yx} - K_{xy}}{2} & 0 \end{pmatrix} \qquad (6)$$

Where K_{sym} and K_{asym} represent the conservative and curl component, respectively With the stiffness measured at the hand and the postural geometry, the joint stiffness can also be calibrated. The joint stiffness is given by a torque-angular displacement relation and the transformation from hand stiffness to joint stiffness is achieved by applying the transform from hand velocities (δy, δx) to joint velocities ($\delta\theta_1$, $\delta\theta_1+\delta\theta_2$).

$$\begin{pmatrix} \delta x \\ \delta y \end{pmatrix} := J \cdot \begin{pmatrix} \delta\theta_1 \\ \delta\theta_1 + \delta\theta_2 \end{pmatrix} \tag{7}$$

J is the function that transforms angular joint velocity to end-point velocity. From Eqn. 2

$$J := \begin{bmatrix} \left(L_1 \cdot \sin(\theta_1) + L_2 \cdot \sin(\theta_1 + \theta_2)\right) & L_2 \cdot \sin(\theta_1 + \theta_2) \\ -\left(L_1 \cdot \cos(\theta_1) + L_2 \cdot \cos(\theta_1 + \theta_2)\right) & -L_2 \cdot \cos(\theta_1 + \theta_2) \end{bmatrix} \tag{8}$$

The joint stiffness, R, can then be calculated with.

$$R := J^T \cdot K \cdot J \tag{9}$$

$$R := \begin{pmatrix} R_s + R_t & R_t \\ R_t & R_e + R_t \end{pmatrix}$$

R_s, R_e are the monoarticular shoulder and elbow stiffness (see Figure 2), and R_t is the biarticular stiffness.

3.0 Experimental Procedure:

3.1 Apparatus:

Subjects were seated with their shoulder and torso restrained by a four-point harness belt and so that their right, dominant hand comfortably gripped the handle of an arm support assembly located at the end of a two-link planar manipulandum. The arm support assembly comprised a handle that was co-located to the free end of the two-link manipulandum and rotated freely about the axis perpendicular to the plane of the manipulandum, and a padded support that extended below the subject's forearm to support the elbow in the horizontal plane. This gave the subject's arm a free range of motion in the plane of the manipulandum and fixed the center of his hand at the end of the two-link manipulandum.

An InMotion Inc robotic manipulandum, model 2 was mounted onto a table such that the plane of the manipulandum was perpendicular to the direction of $\hat{\mathbf{g}}$ (the gravity field). Two torque motors mounted to the base of the apparatus and connected independently to each mechanical joint of the manipulandum, permitted application of forces of controlled direction and amplitude to the handle. Position transducers co-located on the motors permitted measurements of the position of the handle of the manipulandum to within meters, and a force transducer mounted at the handle and permitted measurements of the force experienced at the handle to within 1e-3N. An LCD screen mounted on an adjustable support was positioned at eye level (approximately 0.3 m above the plane of the manipulandum for a seated subject) and between the subject and the origin of the apparatus (the intersection of the axis of rotation of the torque motors with the horizontal plane of the manipulandum). This was used to display real-time images representing the hand's position in the pre-defined workspace. An InMotion Inc robitic manipulandum controller supplied the torque motors with power. A computer located outside of the subject's workspace was connected to the torque motors, position transducers, the force transducer and the LCD screen and recorded all data relevant to this study at 500 hertz. This computer also executed code developed by Olumuyiwa Oni (ME Undergraduate, 2006) and Eric Smith (ME Graduate) that defined the procedures of both the joint stiffness study and the cross-body movement study.

3.2 Experimental Methods:

The position transducers and force transducer were independently calibrated InMotion Inc. The subject was then seated in front of the apparatus and instructed to complete a joint stiffness study and a cross-body movement study.

3.2.1 Preparation

Positioning Subject in Workspace:

Prior to seating the subject, the subject's weight, height, forearm and upper arm lengths, and several circumferential measurements along the arm were recorded. The subject was seated directly in front of the manipulandum with their shoulder and torso restrained by a four-point harness belt. The seat was positioned so that the back post was approximately 1.2 meters from the origin of the manipulandum's coordinate system. The positions of the center of rotation of the subject's shoulder in the manipulandum reference frame was also recorded – this would be used later when describing the arm kinematics in the subjects reference frame.

3.2.2 Measuring Subject Postural Stiffness:

Six static targets were located in the workspace and their position was given in the in the reference frame of the manipulandum – with the origin at the intersection between the axis of rotation of the torque motors and the horizontal plane of the workspace. These actual locations can be referred to here as "reference" (11 mm, -9 mm), "left" (-129 mm, 115 mm), 'right" (140 mm, -108 mm),"above left" (-127 mm, 124 mm), "distal" (5 mm, 129 mm) and "above right" (141 mm, 130 mm). The subject was instructed to remain relaxed. As soon as the computer program running stiffness study starts, the first target appears on the screen. The manipulandum apparatus was set so that the hand's position in the workspace corresponded to a yellow dot on the screen, and the target corresponded to a larger, green dot on the screen. The subject was instructed to drag the yellow dot into the green dot, and, once there, to remain relaxed. Once the subject had remained in the target for 1 second, both the target and the guide dot were erased from the visual display. After 500 ms, a 1N or 1.6N step in force was applied in a controlled direction to the hand, from the manipulandum. A small damping was also applied to make the imposed movement of the hand was sufficiently damped to minimize the duration of oscillations as the hand returned to rest. The duration of the force was 500 ms. The force at the handle was then reset to zero for 500 ms to allow the subject arm to come to rest. After this period, a second force in different controlled direction was applied to the hand. This process of applying a force step at the handle, then removing it continued until 8 different forces, 45% apart had been applied to the hand at rest at the target. When the 8^{th} force step was removed from the handle, the second target appeared and the subject executed an analogous procedure. Throughout this process force, position data was continuously recorded. Typical displacement imposed by 1N step applied at the handle is shown in Figure 4.

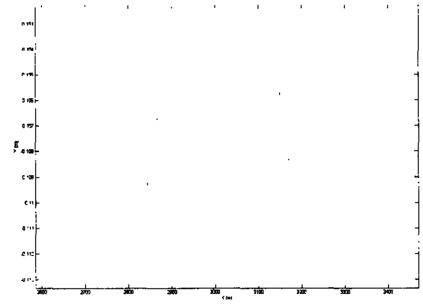

Figure 4. Imposed Displacement.

Data Processing:
A standard least-squares linear regression is used to solve the over-constrained matrix division shown in Eq. 10 and yields a numerical estimate for the coefficients of K.

$$K := \frac{\delta F}{\delta X} \tag{10}$$

There is a minimum requirement on the number of inputs to the regression to yield a reasonable estimate. For example, a single force-displacement input is inadequate to approximate a workspace with motion in two degrees. Generally, the more inputs there are with unique directions, the better the estimate of 2-D stiffness.

In order to get valid least-square estimates of 2-D stiffness two other data filters were applied to the recorded data set.

3.2.3 Measuring Subject Cross-body Movements:

Subject Cross-body Movements was conducted in the same sitting with the Subject Stiffness Study and used the same apparatus. A new set of targets were organized into cross-body pairs – target pairs that required the subject hand to reach across his body and back in the course of landing in the target zones.

4.0 Results:

4.1 Validity of the Stiffness Measurements:

The multi-joint stiffness of the hand was approximated with least-squares fit of the forces applied at a given posture and the resulting displacement. For each study case, all hand positions with fewer than 6 force inputs with unique direction were automatically discarded; this was done to minimize the error associated with the least squares approximation. As a result of this requirement, three postural measurements were discarded, see Table 1.

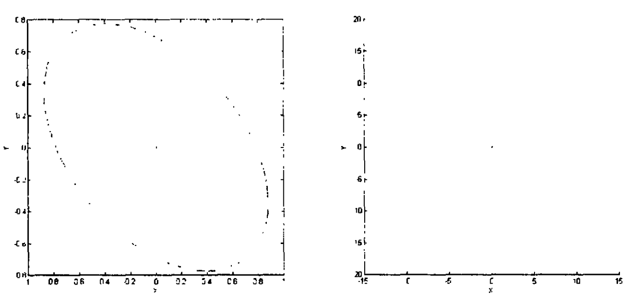

Figure 5. Stiffness Matrix (left) contrasted with measured force-displacement vectors. The major axic of the ellipse corresponds to the more stiff direction for that posture.

In order to verify the stiffness matrix fits, we back-calculated the generation forces necessary to produce the measured displacements by plugging the calculated stiffness and measured hand displacement into Eqn (10) The magnitude and direction of the calculated generation forces were then compared to the measured generation forces for the same displacements. The visual comparison of the forces can be seen in Figure 6. The vectors plotted represent the measured generation forces (red) and the calculated generation forces (blue). The center of the figure, located by a star, represents the equilibrium posture. The position of the proximal end of the generation force, relative to the equilibrium posture is equivalent to the distance and direction of the displacement from equilibrium position that it imposed on the hand. Valid measurements of stiffness should produce force vectors equivalent in direction and magnitude to the measured force vectors. Visually, the small angle between the measured (red) and the predicted forces (blue) indicated that the symmetric stiffness matrix is a god approximation of the force displacement characters of the limb.

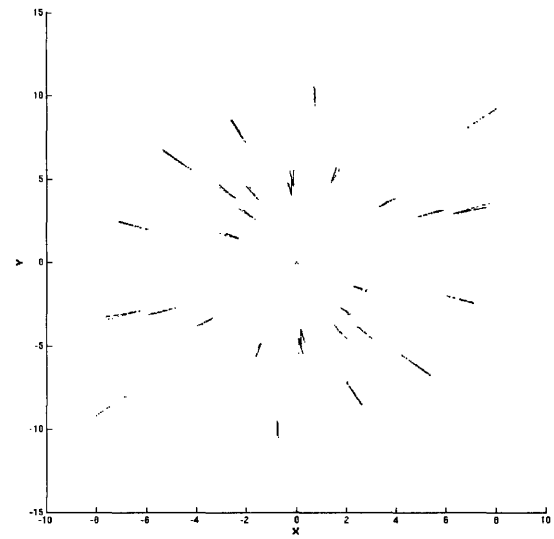

Figure 6. Stiffness Matrix (left) contrasted with measured force-displacement vectors. The major axic of the ellipse corresponds to the more stiff direction for that posture.

Measurements of Ataxic Hand Stiffness and Normal Hand Stiffness Comparable:

Table 1: Postural Hand Stiffness and Joint Stiff given for targets

Subject	Hand Position	Hand Stiffness		Joint Stiffness	
Normal Subject	Reference	319.83	-91.194	57.56	22.847
		-104.62	265.65	21.365	24.442
	Left	543.05	7.9704	85.402	43.661
		-25.304	331.82	40.009	45.91
	Right	320.29	-4.2159	141.66	76.632
		5.8339	515.61	77.313	47.166
	Above Left	528.04	31.957	213.67	114.34
		154.53	702.21	124.53	78.481
	Distal	483.66	275.19	165.25	105.78
		219.13	650.98	101.13	75.346
	Above Right	268.07	1.2377	80.294	40.497
		38.301	224.98	44.63	31.842
Ataxic Subject	Reference	167.88	-233.99	31.486	16.517
		-231.96	725.08	16.517	8.6648
	Left	442.75	-48.936	71.754	33.421
		5.8304	321.24	38.474	34.826
	Right	N/A	N/A	N/A	N/A
		N/A	N/A	N/A	N/A
	Above Left	152.95	-1.8951	57.68	30.258
		15.686	209.54	30.258	15.873
	Distal				
	Above Right	N/A	N/A	N/A	N/A
		N/A	N/A	N/A	N/A

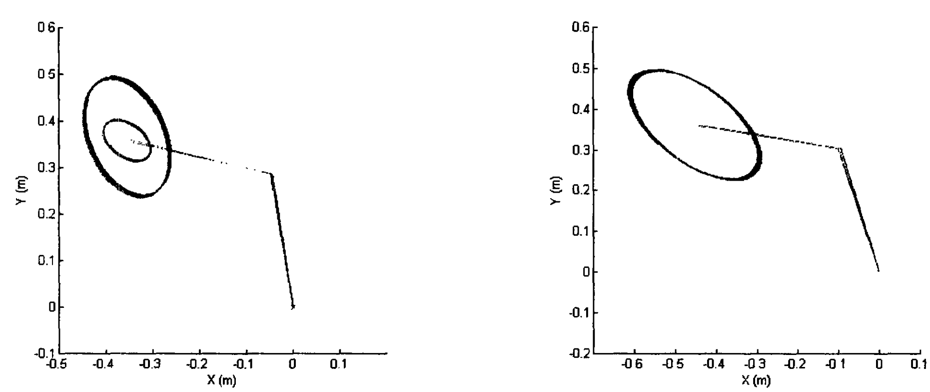

.Figure 7. (Left) Stiffness Ellipses for ataxic subject for maximal (larger magnitude ellipse) and minimal co-activation at position “Left”. (Right) Stiffness Ellipses for a normal subject for maximal (larger magnitude ellipse) and minimal co-activation at position “Left”.

The representations of postural hand stiffness of the ataxic and normal subjects are shown in Figure 7 and Figure 8.

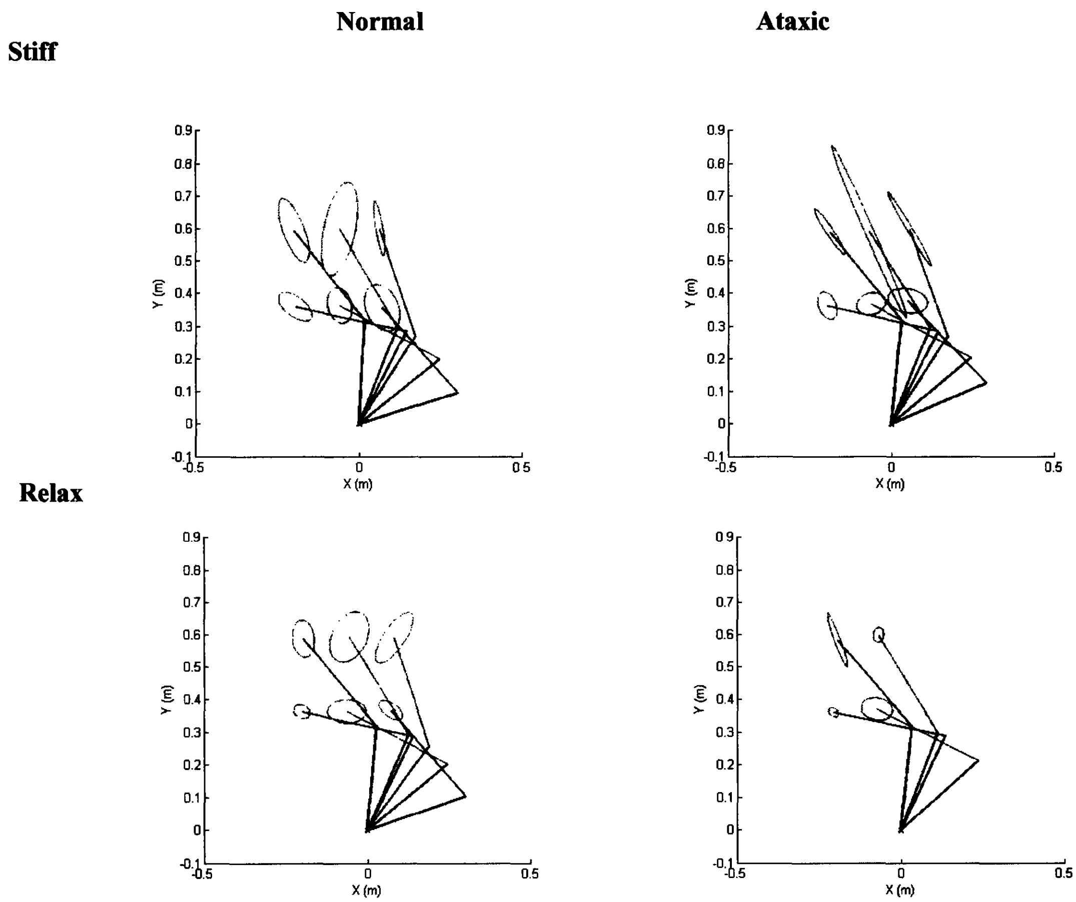

Figure 8. Stiffness Ellipse Variation for Normal Subject Stiff (left top); Normal Subject Relaxed (left bottom); Ataxic Subject Stiff (left top); Ataxic Subject Relaxed (left bottom);

Conservative Stiffness is Dominant:

By applying Eqn(5) to the calculated hand stiffness matrix, matrices representing the symmetric and asymmetric stiffnesses of the hand were calculated. These matrices respectively represent the conservative and non-conservative generation forces. With applying a procedure similar as to when validating the measurement technique for the hand stiffness, we determined that the stiffness matrix is largely conservative. Visual comparison, see Figure 9, of the conservative generation forces comprised the majority of the observed generation forces throughout the study. The contribution of curl to the force-displacement response of the hand can be justifiably neglected. As shown in Table N, the magnitude of curl is .... This is consistent with results obtained by Hogan, Mussa-Ivaldi. A non-negligible curl would be indicative of path dependent energy dissipation/generation during movements around closed paths; this can not exist in a purely elastic force field.

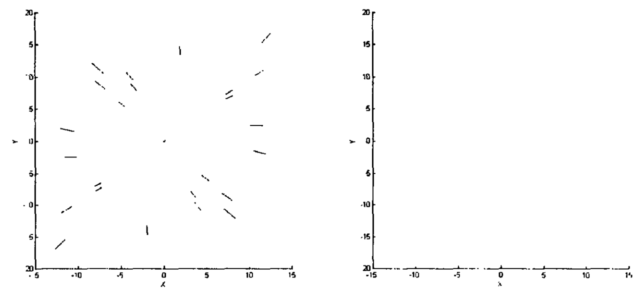

Figure 9: The symmetric representation of the hand stiffness was compared

Table 2:

Subject	Hand Position	Curl	Kmax	Eccentricity	Offset Angle
Normal Subject	Reference	22.106	394.11	0.87418	-35.372
	Left	41.835	542.09	0.7894	2.1708
	Right	76.973	515.48	0.78335	268.29
	Above Left	119.44	727.03	0.72174	232.17
	Distal	103.45	826.75	0.92806	237.43
	Above Right	42.563	269.15	0.5549	1.6052
Ataxic Subject	Reference	16.517	809.65	0.99469	-70.129
	Left	35.947	440.35	0.67814	-22.334
	Right	N/A	N/A	N/A	N/A
	Above Left	30.258	209.01	0.67879	254.37
	Distal				
	Above Right	N/A	N/A	N/A	N/A

Results Comparable to Mussa-Ivaldi Study:

The range of both the joint stiffnesses and the postural hand stiffness for the Ataxic subject are comparable to Mussa-Ivaldi results. The observed joint stiffnesses and the postural hand stiffness for the normal subject were roughly twice the magnitude reported by Mussa-Ivaldi. The orientation of stiffness ellipses, however, was consistent with Mussa-Ivaldi results for similar workspace postures. See Table 2.

Table 3.

Subject	Joint Stiffness	Relaxed Posture	Stiff Posture
Normal Subject	Shoulder Joint Stiffness (R11)	45.7 ± 21.1	48.2 ± 20.0
	Elbow Joint Stiffness (R22)	-8.3 ± 29.6	1.2 ± 18
	Bi-articular Stiffness (R12)	51.3 ± 34.0	51.1 ± 44.0
Ataxic Subject	Shoulder Joint Stiffness (R11)	25.0 ± 9.6	23.5 ± 13.6
	Elbow Joint Stiffness (R22)	-5.7 ± 3.6	-3.0 ± 1.2
	Bi-articular Stiffness (R12)	28.2 ± 16.2	29.1 ± 16.2

4.2 Cross-body Movements:

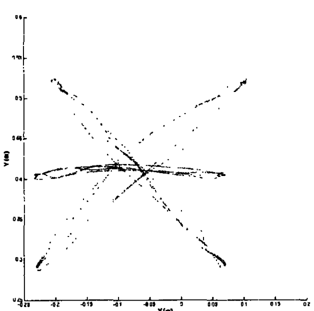

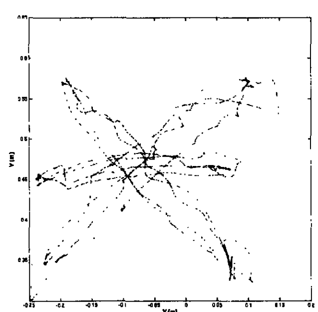

The cross-body movements of the ataxic and normal subject showed significantly different hand trajectories. In both scenarios depicted, the subject was instructed to complete the point-to-point cross-body movements slowly. Qualitatively, the movements of the normal subject are smooth. Also, the overlap of the trajectories over two independent runs is fairly high. Conversely, the ataxic cross-body movements are very jagged and show very little overlap. In addition, the overshoot in the ataxic hand trajectory is more dramatic than for the normal trajectory.

5.0 **Discussion:**

From Table 1 and Figure 8 we observed that the postural hand and joint stiffnesses calculated for the ataxic and normal subject were similar. They show similar maximal stiffness orientations, and similar maximum-minimum stiffness rations. Conversely, the hand trajectories observed during cross-body movements are vastly different. It seems clear that the symmetric stiffness calculated does not sufficiently explain this difference. More rigorous studies are necessary

Because the joint stiffness of the ataxic subject was comparable to the stiffnesses measured for the Normal subject, and those reported by Mussa-Ivaldi, it is clear that the deficiency of controlled kinematic behavior in ataxic hand trajectory cannot be described by measurements of stiffness. It is important to make clear that the measurements of stiffness take into account both the contribution by the mechanical stiffness of the muscle-limb body and the reflex response of the CNS to external forces. Taken together,

5.1 Error Analysis:

Though the technique used to calculate multi-joint postural stiffness produced results that demonstrated a good fit, many data points had to be thrown out because of subject position corrections during force application. Less than 15% of the time required to apply a set of step input forces to a hand at an equilibrium position yielded useful results. As we prepare to build on this study, we find it critical to change our approach to measuring stiffness from one of applying forces and measuring displacements, to one of applying a displacement and measuring the generated force. The latter strategy will require less time for each measurement performed, and can curb the affect of subject position correction on measurement errors.

References:

Flash T (1987) The control of hand equilibrium trajectories in multi-joint arm movements. Biol Cybern 57: 257-274

Frolov AA, Dufosse M, Rizek S, Kaladjian A (2000) On the possibility of linear modeling the human arm neuromuscular apparatus. Biol Cybern 82: 499-515

Gomi H, Kawato M (1997) Human arm stiffness and equilibrium-point trajectory during multi-joint movement. Biol. Cybern. 76: 163-171

Hwang EJ, Smith MA, Shadmehr R (2006) Adaptation and generalization in acceleration-dependent force fields. Exp Brain Res 169: 496-506

Kawato M, Gomi H (1997) A computational model of four regions of the cerebellum based on feedback-error learning. Biol. Cybern. 68: 95-103

Lan N (1995) Analysis of an optimal control model of multi-joint arm movements. Biol. Cybern. 76: 107-117

Mah CD (2001) Spatial and temporal modulation of joint stiffness during multi-joint movement. Exp Brain Res 136: 492–506

Mussa-lvaldi FA, Hogan N, Bivi E (1985) Neural, mechanical and geometric factors subserving arm posture in humans. J Neurosci Vol. 5, No. 10: 2732-2743

McIntyre J, Mussa-lvaldi FA, Bizzi E (1989) Modeling of Multi-Joint Motor System. IEEE Engineering in Medicine & Biology Society 11th Annual International Conference.

Shadmehr R, Mussa-Ivaldi FA, Bizzi E (1993) Postural force fields of the human arm and their role in generating multi-joint movements. J Neurosci 13:45–62